Magnetic Control of Plasma Arc Welding (Report III)† —On the Pressure Distribution of Plasma and its Effect on Key-Hole Action—

Yoshiaki ARATA*, Hiroshi MARUO, Yoshinori HIRATA*** and Yasuyuki HORIO******

Abstract

When the cusp type magnetic field is imposed on the plasma arc, its cross section becomes oval. By this magnetic control, feasible range for key-hole welding is expanded markedly. Key-hole is, however, observed to be larger than conventional one. In order to make clear this phenomena, plasma arc pressure and pressure due to surface tension of molten metal are taken into account to determine the equilibrium key-hole diameter.

Calculated value agrees with experimental results.

1. Introduction

In an ordinary plasma arc welding of medium thick plate, key-hole technique is widely used. Key-hole formation is, however, not always stable, but is fairly sensitive to any change of welding conditions such as arc current, working gas flow rate, traveling velocity and so on. At the same time, bead formation in a key-hole process depends on the intrinsic physical properties of material to be welded such as surface tension, viscosity and density of molten metal at elevated temperature.

In general, feasible range of welding operation for thicker plate exceeds 9 mm is comparative narrow to that for medium thick plate of around 6 mm. Burn-through or lack of penetration will often come arise from small fluctuation of welding parameter.

As described in our previous report,[1), 2)] on the other hand, when cusp magnetic field imposed to the plasma arc, feasible range of welding operation could be broadened markedly, and narrow, deep penetrated weld bead was obtained as a result of magnetic deformation of arc plasma. It was also pointed out then to be formed somewhat larger key-hole than that in ordinary plasma welding process.

Presented in this paper are series of analysis on the relation between the pressure of plasma arc at the key-hole region and the diameter of key-hole.

2. Experimental Apparatus and Materials

Plasma arc torch system used in present investigation is composed of ordinary plasma torch, electromagnets to generate a cusp typed magnetic field and auxiliary shield cover. The torch and electromagnets used are almost the same with those in previous report. Their structures are as shown in **Fig. 1** and **Fig. 2.** The pole pieces of magnet were made of soft iron, 1 mm in thickness, and magnetic flux density obtained with field coil current of 3 amp. was about 300 gauss at the site located 5 mm from the nose of pole piece. Field strength varies proportionally as field coil current not exceeds 3 ampare.

Nozzle diameter of plasma torch was 3 mm and arc current was changed over a range from 100A to 200A. Argon was chiefly employed both for plasma working gas and shield gas. Materials used in welding experiment were 304 type stainless steel plate, 6 mm and 9 mm in thickness.

For the pressure measurement of plasma arc on the flat anode plate, a water-cooled copper anode having a pressure tap tube (0.5 mm in diameter) was used. Furthermore, special copper anode having a "key-hole" simulated to the practical one was employed in order to know the actual pressure acting upon the key-hole and neighborhood of them.

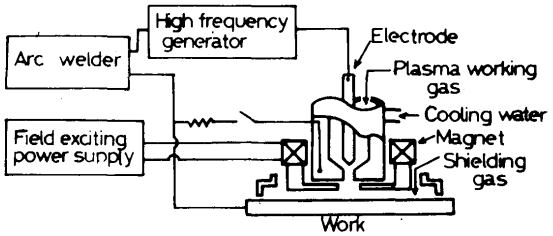

Fig. 1. Schematic diagram of magnetic control of plasma arc.

† Received on July 13, 1974 (IIW Doc. IV-152-74)

* Professor

** Associate Professor, Dept. of Welding Engineering, Faculty of Engineering, Osaka University

*** Graduate Student, Faculty of Engineering, Osaka University

**** KAIGAI Electronic Technical Laboratory

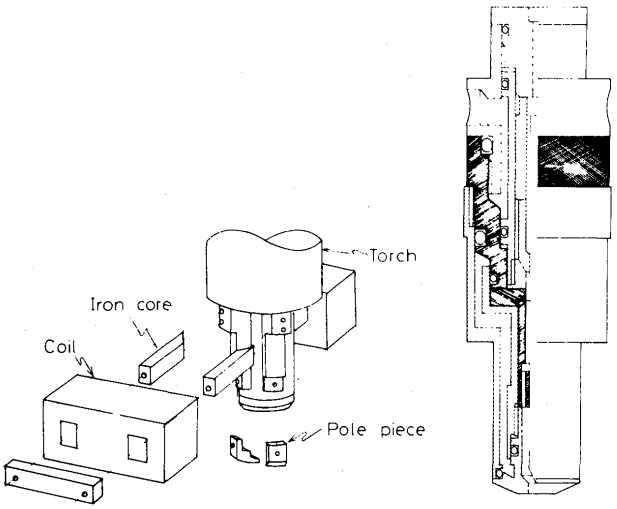

Fig. 2. Electromagnets and plasma arc torch.

3. Experimental Results and Discussion

3.1 Magnetic control of plasma arc with cusp magnetic field

Typical deformation of plasma arc in a cusp type magnetic field is as shown in **Photo. 1.** Each picture of them was taken at the same moment from both direction, longitudinal and transverse. It will be found that the plasma arc column was restricted from both sides and expanded somewhat to the perpendicular direction, and its cross section has deformed to an elliptical as a result. When the working gas flow rate is low, deformation of plasma column can be clearly recognized, but measurement of current flowing into the anode indicated that its cross section takes an oval shape even at the case with higher working gas flows.[2)]

3.2 Feasible range of plasma arc welding

Similarly as described in previous report, all of welding with cusp magnetic field were carried out in key-hole method as well as ordinary one. An example of weld bead made with magnetic field is given in **Photo. 2.** As can be seen in photograph, width of weld bead made by such magnetically controlled plasma arc was fairly narrow comparing with those in conventional method. On the other hand, bottom bead width was observed to be increased rather. It should be noted that undercut free weld bead was obtained even in the case it would be sure to form if no magnetic field was applied.

Consequently, feasible range to give a satisfactory weld has been expanded by an application of magnetic field, as shown in **Fig. 3.**

3.3 Appearances of crater and key-hole

When the cusp magnetic field was applied, weld crater take a distinctive feature and fairly different from those in conventional process. Its front solid wall descends by easier grade and falls into the key-hole. All of molten metal at the front portion were swept away towards rear side of crater in a similar manner as observed in conventional plasma welding,

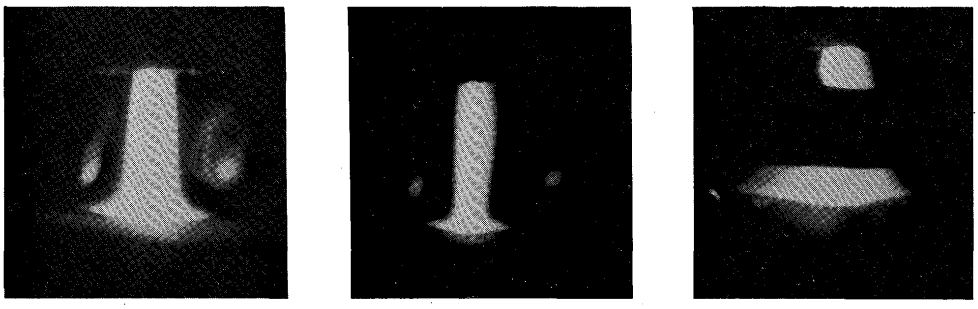

(a) (b) (c)

Photo. 1. Appearances of plasma arc, 150 A, 41 V, 13 mm.
(a) I_f; 0 A (b), (c) I_f; 3 A.

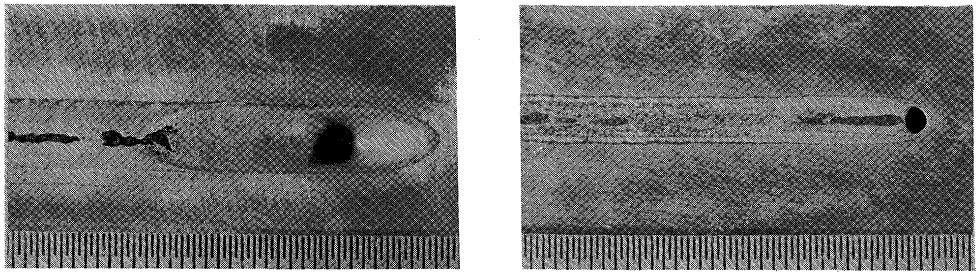

Photo. 2. Weld bead made by magnetic control of plasma, 304 Stainless Steel, 6 mm, 150 A, 35 V, 20 cm/min, I_f 3 A, 4 l/min Argon.

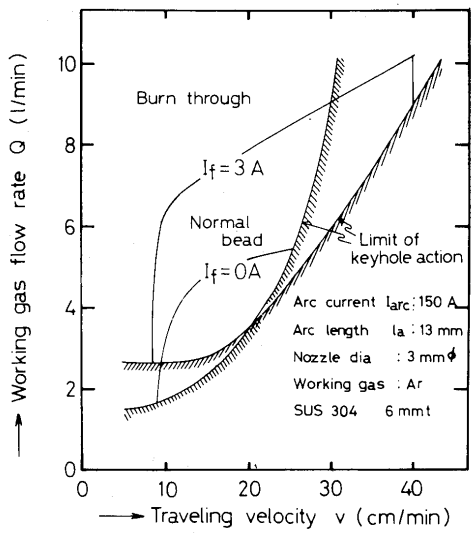

Fig. 3. Feasible range of key-hole welding for both plasma.

but they formed a long tailed oval molten puddle.

Diameter of key-hole was observed to increase certainly whenever magnetic field was applied. Its diameter was determined by taking a photograph of effluent plasma through out the key-hole. **Figure 4** and **5** give the change of key-hole diameter when the

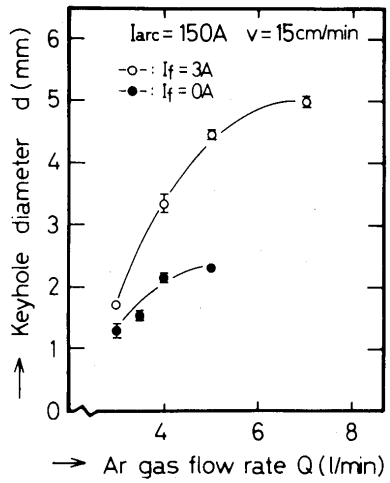

Fig. 4. Effect of working gas flow rate on key-hole diameter.

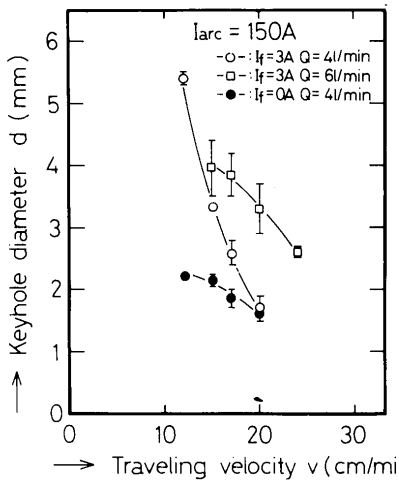

Fig. 5. Effect of welding speed on key-hole diameter.

working gas flow rate or traveling velocity was altered.

Schematic illustration of longitudinal cross section of weld bead is given in **Fig. 6.** Solid-liquid interface could be determined by removing the molten metal. This was carried out by impinging heavy weight hummer upon the work piece so as to rotate it very quickly.

The experiment showed that the heat input per unit length of weld does not so much change the length of crater, λ_0. It, however, prolonged certainly by an application of magnetic field, as shown in **Fig. 7.**

Most closest diameter of "solid" wall around the the key-hole, d_0, was observed to be remained unchanged, while key-hole diameter changed in response to the welding parameter as mentioned above.

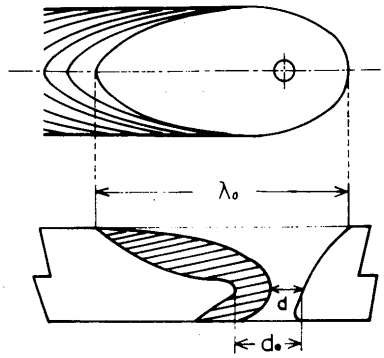

Fig. 6. Longitudinal cross section of molten pool.

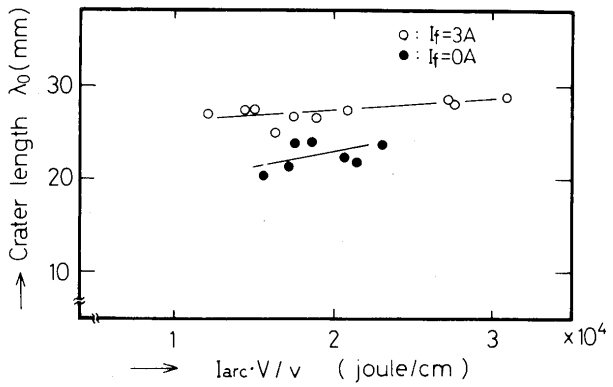

Fig. 7. Relationship between heat input and length of crater.

3.4 Dynamic pressure due to plasma arc

When the fully penetrated key-hole welding is progressing, certain balance should be established at the bottom of weld bead among the forces acting upon the molten metal. They are upward force due to surface tension of liquid metal, downward gravity force, and dynamic force due to plasma stream.

Balance of these forces is, in principle, very delicate, and each force is also influenced by many factors.

Figure 8 shows an experimental result obtained in the measurement of pressure due to plasma arc, which was carried out with devices as shown in **Fig. 9.** The effect of magnetic field is seen more clearly when the working gas flow rate is relative low. When the gas flow rate became higher, difference could be hardly seen. Their peak value increased, of course, with working gas flows.

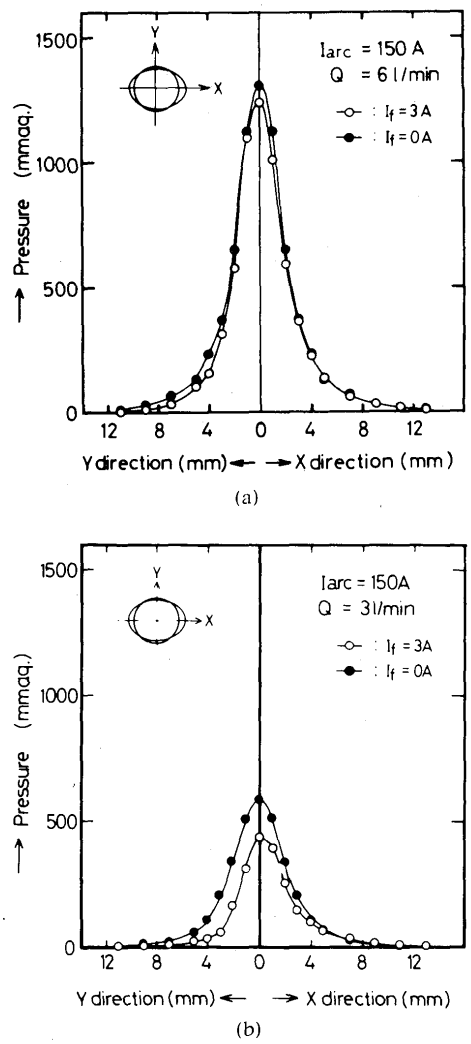

Fig. 8. Pressure distribution on the flat anode.

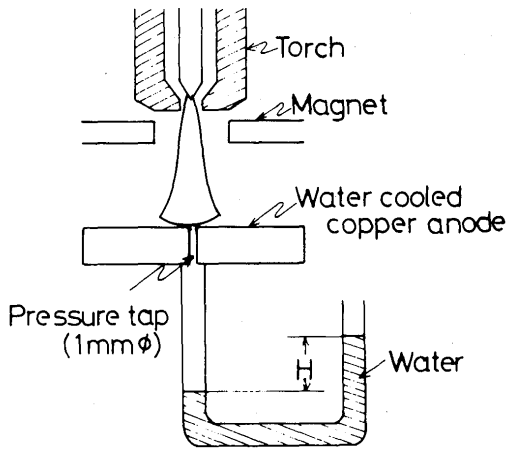

Fig. 9. Dynamic pressure measurement devices.

These results are, however, obtained with flat anode, and is insufficient to elucidate the reasons why large diameter of key-hole is formed by an application of magnetic field.

In order to know actual pressure distribution while the key-hole is formed, another experiment was carried out using water cooled copper anode having a simulated key-hole. Cross-section of this anode plate is shown in **Fig. 10.**

In practical welding, axis of torch and center of key-hole does not meet each other, and torch is usually shifting forward some distance. So, measurement was made by changing the distance of torch axis measured relative to that of key-hole, ξ, in steps. Diameter of key-hole was also changed as 0, 1, 2, 3 and 5 mmϕ.

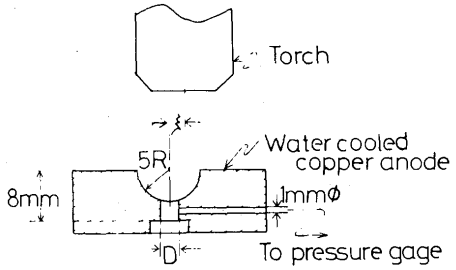

Fig. 10. Water cooled copper anode for the measurement of static pressure at the key-hole.

In **Fig. 11** is given the results obtained for the case that key-hole is not formed. Stagnation pressure at the center of crater is seemed to decrease by an application of magnetic field. As can be seen in lower range of working gas flows in Fig. 3, key-hole is still formed if no magnetic field is applied. For this reason, it will be sufficient to consider only stagnation pressure.

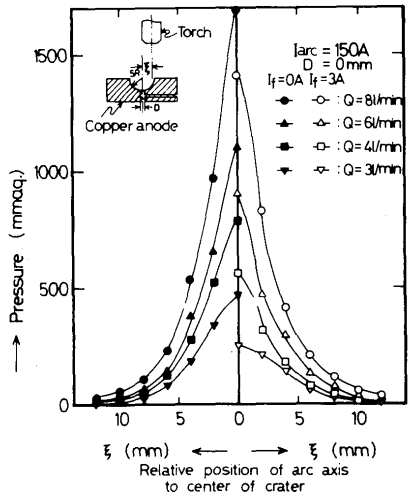

Fig. 11. Relationship between positioning of arc and total pressure at the bottom of crater.

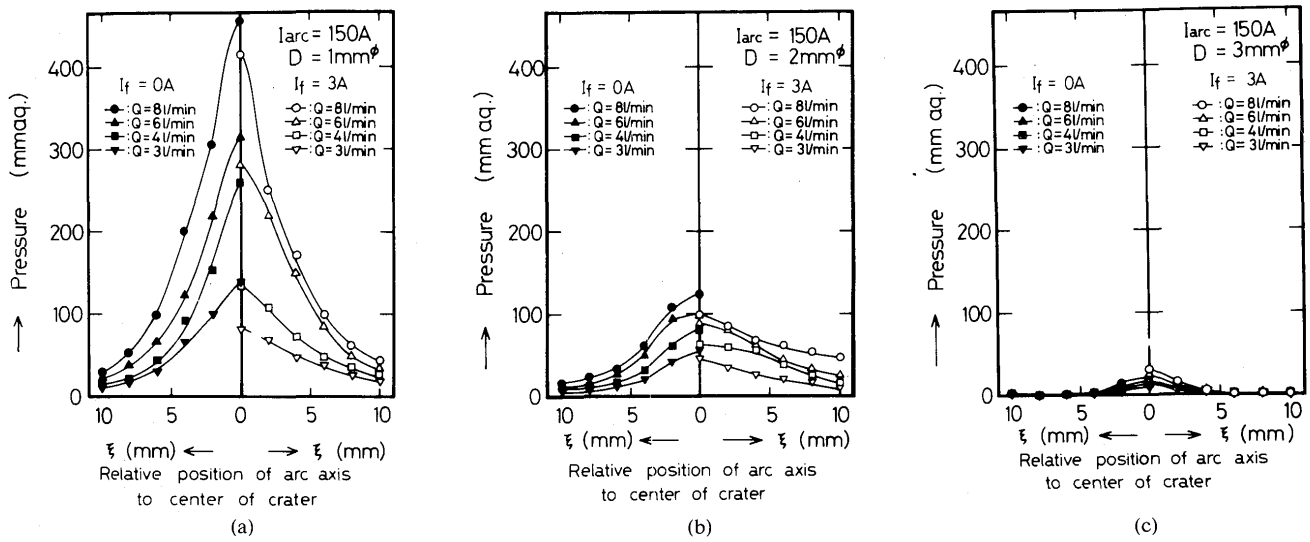

Fig. 12. Effect of arc positioning and key-hole diameter on static pressure at the key-hole.

Static pressure at the midpoint of key-hole was measured for various diameter of key-hole, and effect of lag distance (ξ) on static pressure was investigated. Experimental results are summarized as **Fig. 12.** Static pressure increased with working gas flow rate, but decreased rapidly as a diameter became larger. In present experiment, static pressure was no longer appreciable when diameter of key-hole exceed 3 mm.

As obvious from these results, lag distance, ξ, has much effects on the static pressure at the key-hole region. When the lag distance is not so large, static pressure inside of key-hole produced by ordinary plasma arc is higher than those of magnetized plasma arc, but this correlation is the reverse for the larger value of ξ as shown in **Fig. 13.** This characteristics plays an important role on occasion to determine the key-hole diameter, as described later.

In order to evaluate the actual pressure act on molten pool, similar measurements were carried out.

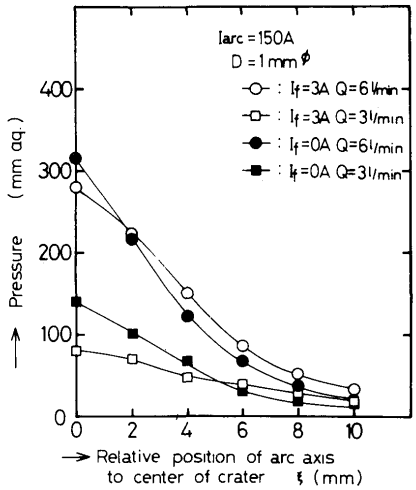

Fig. 13. Relation between static pressure and arc position.

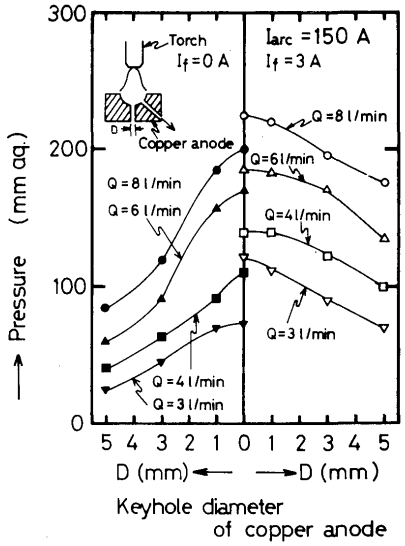

Fig. 14. Dynamic pressure act on molten pool.

Its result is represented in **Fig. 14.** In this experiment, plasma torch was set just above the key-hole. It was found that pressure act on molten pool was enhanced by an application of magnetic field, and this trend was confirmed at any key-hole diameter. These strong pressure would be produced by the change of plasma stream as a result of magnetic constriction.

Relationship between key-hole diameter and static pressure inside key-hole is as shown in **Fig. 15.**

3.5 Pressure due to surface tension of molten metal

As described in former section, it is presumed that molten metal is sustained by the balance of forces, which are dynamic force of plasma stream, gravity head and pressure difference at the surface of molten metal due to surface tension.

If key-hole is assumed to be hollow cylinder

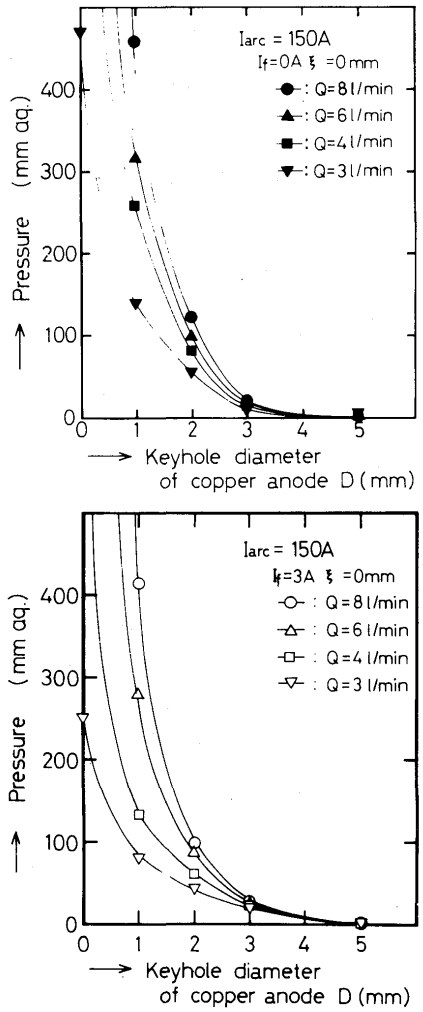

Fig. 15. Effect of key-hole diameter of copper anode on the static pressure of key-hole plasma.

having a diameter of d, difference of internal pressure ΔP is given after Laplace equation,

$$\Delta P = \gamma\left(\frac{1}{R_1} + \frac{1}{R_2}\right) \tag{1}$$

ΔP: Difference of internal pressure

γ: Surface tension

R_1, R_2: Radii of curvature at the point referred, which are perpendicular each other

Substituting $R_1 = d/2$ and $R_2 = \infty$ to above equation (1), following relation is obtained.

$$\Delta P = \frac{2\gamma}{d} \tag{1'}$$

From equation (1'), it is easily deduced that if the diameter of key-hole, d, becomes larger, the static pressure of plasma stream becomes inversely small, which is necessary to balance with ΔP. Actual key-hole is not, of course, hollow cylinder, but likely to be such shape as in Fig. 6. Then, it may possible to consider the model as shown in **Fig. 16,** and we

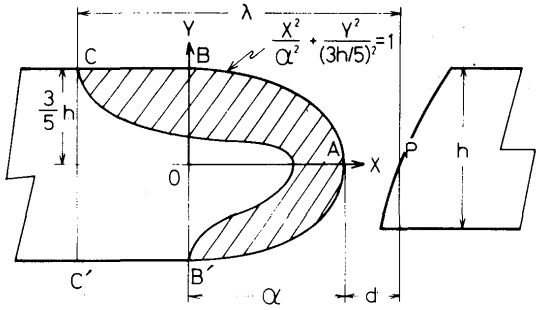

Fig. 16. Molten pool model for calculation.

assume that;

1) there is no molten metal at the front area of crater
2) key-hole is always being circle, and its diameter, d
3) envelope of longitudinal cross section of molten metal at the rear part of key-hole is elliptical curve

In Fig. 16, X axis was set at 3h/5, considering real shape of cross-section and bottom bead, too. Surface of molten metal between the lines B–B′ and C–C′ is assumed to be flat.

If length of molten pool, λ, is given, α can be calculated so as to not change the area of CBAB′C′, since volume of molten metal should be ever constant.

If λ is invariant, we can obtain a following equation,

$$\frac{6}{5}h\cdot(\lambda - d - \alpha) + \frac{\pi}{2}\cdot\frac{3}{5}h\cdot\alpha = \frac{\pi}{2}\cdot\frac{3}{5}h\cdot\lambda \tag{2}$$

$$\alpha = \lambda - \frac{4}{4-\pi}d \geqq 0$$

From above equation, we can be obtain a following inequality.

$$0 \leqq d \leqq \frac{4-\pi}{4}\lambda$$

This equation suggest that key-hole diameter, d, has a maximum value with respect to the value of λ, which is corresponding to $\Delta P = 2\gamma/d$ in Eq. (1'). If d is beyond this maximum value, it is no longer easy to maintain the molten metal as it was, and burn through will be occured. This result does not contradict with previous statement, that is, d will take a larger value as λ becomes larger.

Now at a point A in Fig. 16, if its curvatures $1/R_1$, $1/R_2$ are known, internal pressure difference required to maintain the key-hole at a diameter of d can be determined using equation (1).

In general, curvature 1/r of the curve, which is expressed x=f(t) and y=g(t) in x-y coordinate with

parameter t, can be shown as following equation.

$$\frac{1}{r}=\frac{\frac{df}{dt}\cdot\frac{d^2g}{dt^2}-\frac{dg}{dt}\cdot\frac{d^2f}{dt^2}}{\left\{\left(\frac{df}{dt}\right)^2+\left(\frac{dg}{dt}\right)^2\right\}^{\frac{3}{2}}} \quad (3)$$

Then, for the key-hole in Fig. 16, curvatures $1/R_1$, $1/R_2$ can be expressed as follows;

$1/R_1=d/2$, $1/R_2=25\alpha/9h^2$

Using equation (1) and (2), following equation is led.

$$\Delta P=\frac{\gamma}{9(4-\pi)h^2}\cdot\frac{100d^2-25(4-\pi)\lambda d+18(4-\pi)h^2}{d} \quad (4)$$

In **Fig. 17** represented the results calculated for various parameter λ, plate thickness h=6mm, surface tension of molten metal γ=1500 dyne/cm.[3] From this figure, it can be seen that the static pressure necessary to maintain the key-hole of d may be enough low, if length of molten pool λ is so long.

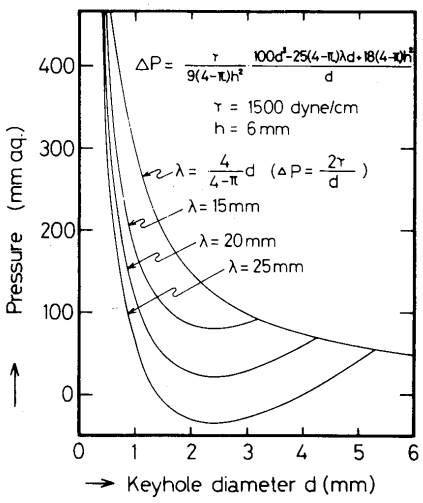

Fig. 17. Pressure due to molten metal calculated.

3.6 Equilibrium diameter of key-hole

Static pressure of plasma stream at the key-hole is already obtained experimentally. Pressure required to maintain the key-hole could be obtained. Then, it becomes possible to consider the equilibrium diameter of key-hole.

For example, if the key-hole is presumed to be a hollow cylinder with a diameter of d, we can find a intersecting point on both curves, as shown in **Fig. 18.** Then it may be possible to consider that the key-hole will be formed at this pressure and with this diameter. If key-hole becomes larger than d*, it will be soon restricted by sorrounding molten metal wall, since

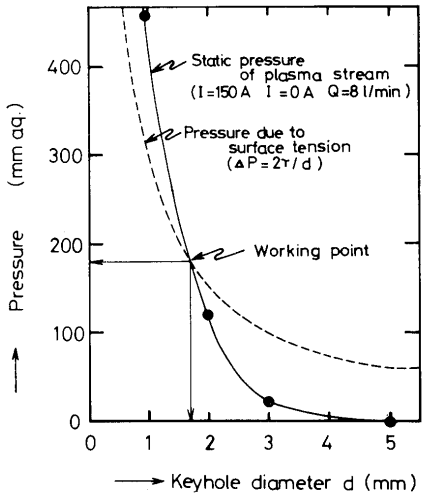

Fig. 18. Pressure due to molten metal calculated.

pressure due to the surface tension exceeds the static pressure of plasma stream. The reverse is also true.

In practical welding, plasma arc torch was in advance of key-hole, and their actual length was measured for both plasma arc processes with and without magnetic control. As can be seen in **Fig. 19,** distance of arc measured relative to the center of key-hole increased almost lineary to the traveling velocity, and usually the arc axis of controled plasma arc located closer to key-hole axis.

The effect of welding parameter on this equilibrium diameter of key-hole is also possible to evaluate.

When the working gas flow rate is altered, key-hole will change its diameter as indicates in **Fig. 20.** From this result, it may be suggested that the key-hole in controlled plasma arc welding would be larger than that in conventional one.

An example of the effect of traveling speed on diameter of key-hole is shown in **Fig. 21.** As the traveling speed becomes fast, key-hole diameter

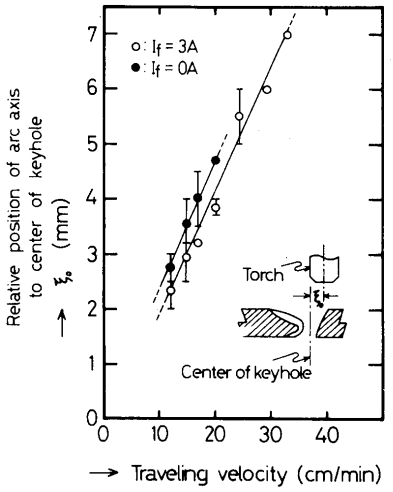

Fig. 19. Position of plasma torch relative to key-hole at various traveling speed.

decreases gradually, but it does not take a continuous value to the point of d=0.

In practical welding, it was observed frequently that the key-hole disappear abruptly after diminishing its diameter to certain value.

Comparison of experimental results and calculated value of key-hole diameter is as shown in **Fig. 22.** Both diameter agree well within a experimental error.

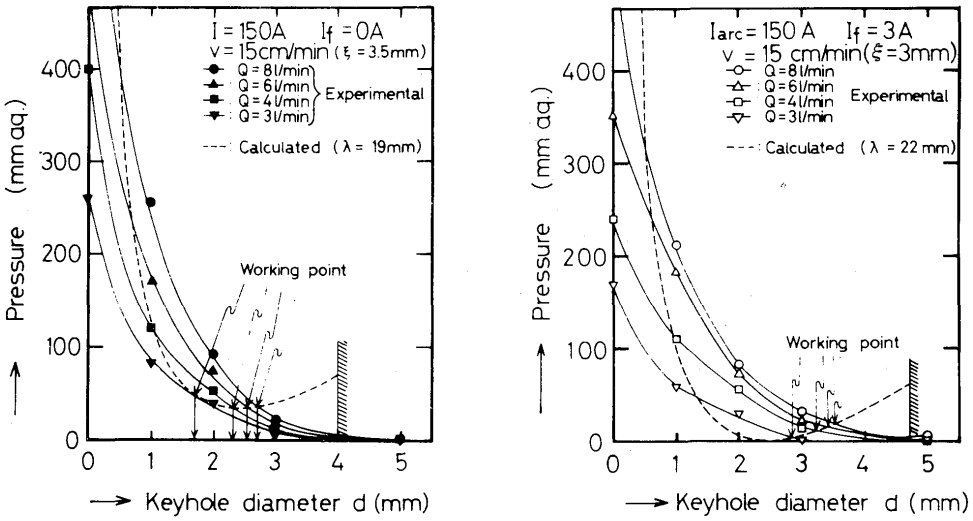

Fig. 20. Determination of key-hole diameter at various working gas flow rate.

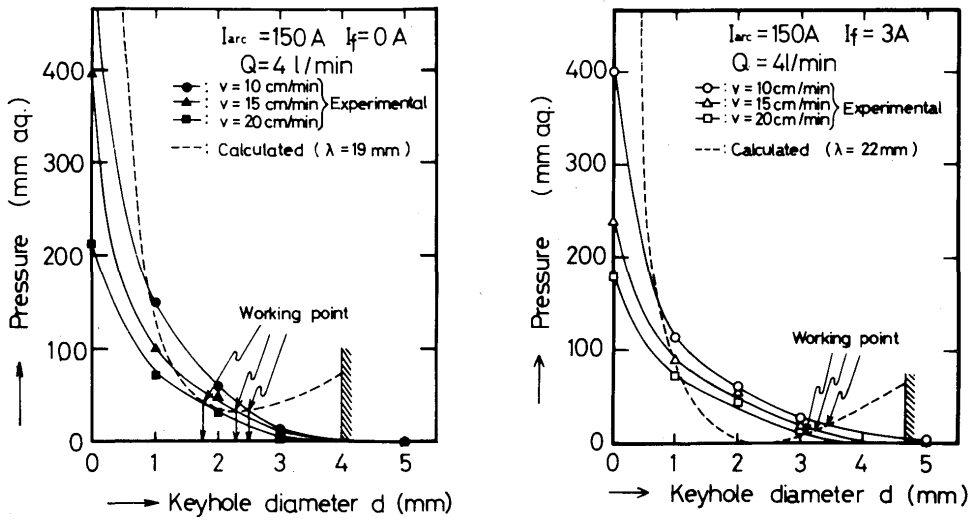

Fig. 21. Determination of key-hole diameter at various traveling speed.

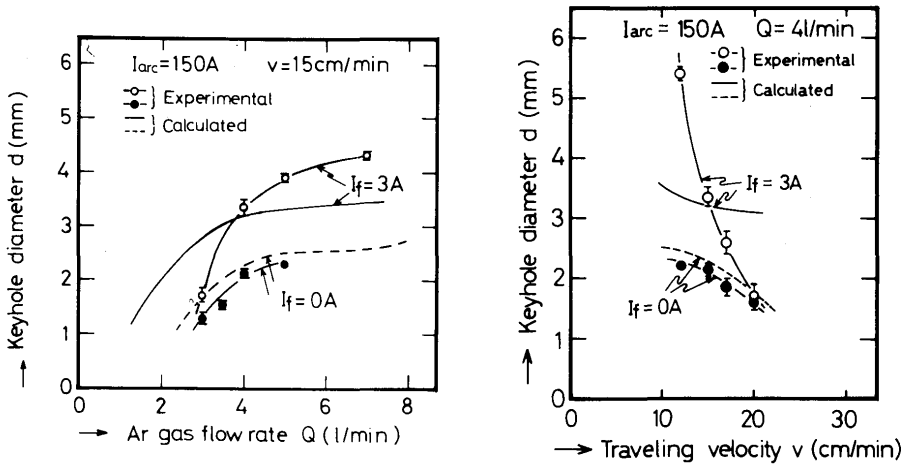

Fig. 22. Comparison of key-hole diameter calculated with experimental value.

4. Conclusion

The results obtained in this series of experiments are summarized as follows;

(1) When the cusp typed magnetic field is imposed on the plasma arc, plasma arc column changes its cross section from circular to oval.
It is possible to weld a stainless steel and others in a key-hole technique with this magnetically controlled plasma arc.

(2) By the magnetic control, feasible range to give a fully penetrated satisfactory weld bead was expanded towards both higher working gas flow rate region and higher traveling velocity side.

(3) No remarkable difference was observed in the total pressure distribution on the flat plane anode, between the both plasma arc processes with or without magnetic field.

(4) Pressure distribution for the case that key-hole was formed was investigated. Static pressure at the key-hole is much influenced by the magnetic field, key-hole diameter and torch positioning relative to the key-hole.

(5) At the key-hole, inward pressure due to surface tension of liquid metal was considered as one of the force to maintain a key-hole.

(6) Equilibrium key-hole diameter was calculated by assuming that pressure due to plasma stream balanced with that due to the surface tension of molten metal.

(7) Effects of working gas flow rate and traveling speed on the diameter of key-hole formed was evaluated. These results agreed well with experimentals.

References

1) Y. Arata and H. Maruo; Magnetic control of arc plasma and its application to welding, Welding in the World, vol. 10 no. 7/8, 1972,
〃 (2nd report) IIW Doc. IV-85-72, 1972.

2) Y. Arata, H. Maruo and K. Yasuda; Some properties of magnetically controlled plasma arc, Transaction JWRI, vol. 2 No. 1, 1973.

3) Franz Cech; A memorandum on surface tension, Preliminary report 71—11.